Behavioral/Cognitive

Distinct Roles of Dopamine Receptor Subtypes in the Nucleus Accumbens during Itch Signal Processing

Tong-Yu Liang,[1,2] **Hua Zhou,**[1] **and Yan-Gang Sun**[1,3]

[1]Institute of Neuroscience, State Key Laboratory of Neuroscience, Center for Excellence in Brain Science and Intelligence Technology, Chinese Academy of Sciences, Shanghai 200031, China, [2]University of Chinese Academy of Sciences, Beijing 100049, China, and [3]Shanghai Center for Brain Science and Brain-Inspired Intelligence Technology, Shanghai 201210, China

Ventral tegmental area (VTA) dopaminergic neurons, which are well known for their central roles in reward and motivation-related behaviors, have been shown to participate in itch processing via their projection to the nucleus accumbens (NAc). However, the functional roles of different dopamine receptor subtypes in subregions of the NAc during itch processing remain unknown. With pharmacological approaches, we found that the blockade of dopamine D1 receptors (D1R), but not dopamine D2 receptors (D2R), in the lateral shell (LaSh) of the NAc impaired pruritogen-induced scratching behavior in male mice. In contrast, pharmacological activation of D2R in both the LaSh and medial shell (MeSh) of the NAc attenuated the scratching behavior induced by pruritogens. Consistently, we found that dopamine release, as detected by a dopamine sensor, was elevated in the LaSh rather than the MeSh of the NAc at the onset of scratching behavior. Furthermore, the elevation of dopamine release in the LaSh of the NAc persisted even though itch-relieving behavior was blocked, suggesting that the dopamine signal in the NAc LaSh represents a motivational component of itch processing. Our study revealed different dynamics of dopamine release that target neurons expressing two dopamine receptors subtypes within different subregions of the NAc, and emphasized that D1R in the LaSh of the NAc is important in itch signal processing.

Key words: **dopamine receptors; itch; nucleus accumbens**

Significance Statement

Dopamine has been implicated in itch signal processing. However, the mechanism underlying the functional role of dopamine in itch processing remains largely unknown. Here, we examined the role of dopamine D1 receptor (D1R) and D2R in the nucleus accumbens (NAc) shell during pruritogen-induced scratching behavior. We demonstrated that D1R in the NAc lateral shell (LaSh) play an important role in motivating itch-induced scratching behavior, while activation of D2R would terminate scratching behavior. Our study revealed the diverse functional roles of dopamine signals in the NAc shell during itch processing.

Introduction

Itch has motivational and affective components (Bautista et al., 2014). Dopaminergic neurons in the ventral tegmental area (VTA) is a major component of the reward system and plays an important role in reward-related and motivation-related behaviors (Bromberg-Martin et al., 2010; Russo and Nestler, 2013; Morales and Margolis, 2017). Human brain imaging studies have implicated the possible role of the dopaminergic system in the affective component of itch (Papoiu et al., 2013; Mochizuki et al., 2014). Recent animal studies have also examined the role of dopamine in itch signal processing (Yuan et al., 2018; Su et al., 2019). Fiber photometry recordings have shown that the activity of dopaminergic neurons in the VTA is correlated with scratching behavior induced by pruritogens. The activity of dopaminergic neurons in the VTA increases after the onset of scratching (Yuan et al., 2018; Su et al., 2019). Behavioral experiments showed that scratching behavior was interrupted by suppressing the activity of dopaminergic neurons in the VTA (Yuan et al., 2018), suggesting that dopaminergic neurons play a modulating role in itch processing. Dopaminergic neurons in the VTA are highly heterogeneous and project to multiple downstream brain areas (Morales and Margolis, 2017). For instance, afferent inputs to

Received Apr. 22, 2022; revised Sep. 20, 2022; accepted Sep. 26, 2022.

Author contributions: Y.-G.S. and T.-Y.L. designed research; Y.-G.S. and H.Z. edited the paper; T.-Y.L. and H.Z. performed research; T.-Y.L. analyzed data; T.-Y.L. wrote the first draft of the paper; T.-Y.L. wrote the paper.

This work was supported by National Natural Science Foundation of China Grants 61890952, 32221003, and 31825013 and the National Science and Technology Innovation 2030 Major Program Grant 2021ZD0204404. Y.-G.S. was supported by Xplorer prize. We thank Dr. Juan Deng for comments on the manuscript, Dr. Yulong Li at Peking University for providing the AAV-hSyn-DIO-EGFP-CAAx virus, and Yan-Jing Zhu for the technical support and all the laboratory members of Y.-G.S. for their helpful discussions.

The authors declare no competing financial interests.

Correspondence should be addressed to Yan-Gang Sun at yangang.sun@ion.ac.cn.

https://doi.org/10.1523/JNEUROSCI.0821-22.2022

the lateral shell of the nucleus accumbens (NAc LaSh) are mainly from the lateral VTA, whereas fibers from the medial VTA terminate in the medial shell of the NAc (NAc MeSh; Lammel et al., 2008; Beier et al., 2015; Yang et al., 2018). Previous studies used fiber photometry to record the calcium signal of dopaminergic fibers from the VTA to different subregions of the NAc and found that the dopaminergic fibers in the NAc LaSh exhibited a more prominent elevation in activity than those in the NAc MeSh during pruritogen-induced scratching behavior (Yuan et al., 2018), indicating that these two subregions play differential roles in itch processing. However, the functional roles of these two subregions in itch processing are still unknown.

Dopamine D1 receptor (D1R) and D2 receptor (D2R) represent two important dopamine receptor subtypes. The functional roles of dopamine receptors in itch have been examined in early behavioral experiments. Pharmacological studies showed that systemic activation of D2R induced dose-dependent scratching behavior in squirrel monkeys, and blockade of both D1R and D2R attenuated the scratching induced by quinpirole (Rosenzweig-Lipson et al., 1994; Pellon et al., 1995). In rats, the scratching behavior induced by intrathecal injection of bombesin or intradermal injection of pruritogens was decreased by the systemic blockade of D1R (Merali and Piggins, 1990), and activation of D2R abolished the pruritic stimulus-induced scratching behavior (Merali and Piggins, 1990; Akimoto and Furuse, 2011). These findings indicate that activation of D1R promotes itch-induced scratching behavior, while D2R activation stops scratching behavior. Although dopamine receptors have been demonstrated to be involved in itch processing, these pharmacological studies did not reveal the action site for dopamine receptors that participated in itch processing. D1R and D2R are highly expressed and mark two major neuronal populations in the NAc (Floresco, 2015; Castro and Bruchas, 2019). These two receptor subtypes in the NAc play important roles in motor behaviors. It has been shown that inhibition of D1R and D2R in the NAc suppressed ambulation (Baldo et al., 2002). Activation of D1R in the NAc increased locomotor activity (Meyer et al., 1993). Activation of D2R in the NAc reduced locomotion (Mogenson and Wu, 1991; Wu et al., 1993). However, the functional role of different subtypes of dopamine receptors in the NAc during itch signal processing remains largely unknown.

In this study, we determined the roles of D1R and D2R in the NAc shell in itch processing. We also examined the dynamics of dopamine release of different subregions in the NAc shell during itch processing. Furthermore, we determined the potential role of dopamine in driving itch-relieving behaviors.

Materials and Methods

Animals

Male C57BL/6J, D1-Cre (MMRRC_030989-UCD), D2-Cre (MMRRC_032108-UCD), D1-Cre/GRPR-Flpo, and D2-Cre/GRPR-Flpo mice were used for experiments. C57BL/6J male mice were ordered from the Shanghai Laboratory Animal Center (SLAC). GRPR-Flpo mice were established as described previously (Liu et al., 2019). All mice were housed up to six mice per cage in an animal room under a 12/12 h light/dark cycle (lights on from 7:00 A.M. to 7:00 P.M.) with *ad libitum* access to food and water. Behavioral tests were conducted in the light phase. All procedures were approved by the Animal Care and Use Committee of the Center for Excellence in Brain Science and Intelligence Technology, Chinese Academy of Sciences, Shanghai, China.

Adeno-associated virus (AAV) virus

AAV-EF1α-fDIO-hChR2(H134R)-mCherry-WPRE-pA (AAV2/9, titer: 4.8×10^{12} vg/ml) and AAV-hEF1α-fDIO-mCherry-WPRE-pA (AAV2/9, titer: 3.82×10^{12} vg/ml) were packaged by Shanghai Taitool Biological. AAV-hSyn-DIO-DA2h (AAV2/9, titer: 9.39×10^{12} vg/ml; Sun et al., 2020) was packaged by Vigene Biosciences. AAV-hSyn-DIO-EGFP-CAAx (AAV2/9, titer: 2.95×10^{13} vg/ml) was provided by Yu-Long Li's lab at Peking University.

Drugs

The D1R antagonist SCH23390, D2R antagonist raclopride, D1R agonist SKF38393, and D2R agonist quinpirole were obtained from Sigma.

Surgery

The surgery was performed as described previously (Yuan et al., 2019; X. J. Chen et al., 2021). To monitor the dynamics of dopamine release in the NAc, AAV-hSyn-DIO-DA2h was injected into the NAc of mice (six to eight weeks old), and experiments were performed two to four weeks after viral injection. Mice were anesthetized with a mixture of xylazine hydrochloride and zoleti (mixture of tiletamine hydrochloride and zalazepam hydrochloride), and body temperature was maintained by a heating blanket. Virus was injected via glass pipettes connected to an air pressure system at a rate of ~30 nl/min. For brain surgery, the head was fixed in a stereotaxic apparatus and mice were injected with 0.2–0.3 μl viral solution into the NAc LaSh [anterior-posterior (AP): +0.98 mm; medial-lateral (ML): −1.75 mm; dorsal-ventral (DV): −4.7 mm] or NAc MeSh (AP: +1.34 mm; ML: −0.5 mm; DV: −4.5 mm), and the pipette was withdrawn 5 min later. For optical fiber implantation, the fiber (diameter: 200 μm; NA: 0.37, Shanghai Zhuen Technology) was implanted above the injected site immediately after virus injection. Dental cement was applied to connect the optic fiber to the skull. For cannula implantation, one week before the experiment, cannulas (0.41 mm in diameter, RWD Life Science) were implanted into the bilateral NAc LaSh (AP: +0.98 mm; ML: ±1.75 mm; DV: −4.7 mm) and attached to the skull with dental cement.

For spinal surgery, mice were fixed by mounting the vertebral column in the stereotaxic apparatus. The cervical or lumbar vertebrae were exposed, and virus was injected into the right side of the spinal cord at four (cervical) or three (lumbar) injection sites (interspaced by 400 μm, 400 nl per site). The pipette was withdrawn 5 min later. After virus injection, a blue LED (Teleopto) was attached above the injected sites with dental cement. The incision was closed with stitches.

After surgery, the animals were allowed to recover from anesthesia on a heating blanket.

Experimental design and statistical analysis

Fiber photometry

AAV-hSyn-DIO-DA2h and AAV-hSyn-DIO-EGFP-CAAx (Li Lab) were injected into the NAc LaSh (AP: +0.98 mm; ML: −1.75 mm; DV: −4.7 mm) or the NAc MeSh (AP: +1.34 mm; ML: −0.5 mm; DV: −4.5 mm). An optic fiber (diameter: 200 μm; NA: 0.37, Shanghai Zhuen Technology) was implanted into the virus-injected site as described previously (Yuan et al., 2019). Mice were handled for 3 d before the photometry experiment. Scratching behavior and fluorescence values were recorded simultaneously at 1000 Hz with the F-scope-G-2 (BiolinkOptics) after intradermal injection of chloroquine (CQ; 200 μg/50 μl, Sigma) and endothelin-1 (ET-1; 25 ng/50 μl) in the nape. Photometry and scratching behavior data were analyzed using MATLAB. First, scratching train onset and offset were identified by custom code (Mu et al., 2017; Yuan et al., 2018) according to the characteristic of scratch trace and then manually adjusted to improve the accuracy for defining the time point of behavior onset or offset. We collected 10 s of noise from the recording system while physically preventing any visual input to the recording optic fiber. For the fluorescence signal, the noise signal of the recording system was subtracted from the recorded fluorescence values, and the resulting fluorescence values in each scratch train were derived. The change in fluorescence values ($\Delta F/F$) in each scratch train was calculated by $(F - F_0)/F_0$, in which F stands for fluorescence values at each time point (−5 to 6 s relative to scratch train onset or −6 to 5 s relative to scratch train offset). F_0 stands for the median fluorescence value during the baseline period (−4 to −2 s relative to scratch train onset). The $\Delta F/F$ values of all scratch trains were heat plotted or then averaged and plotted, with a shaded area indicating SEM.

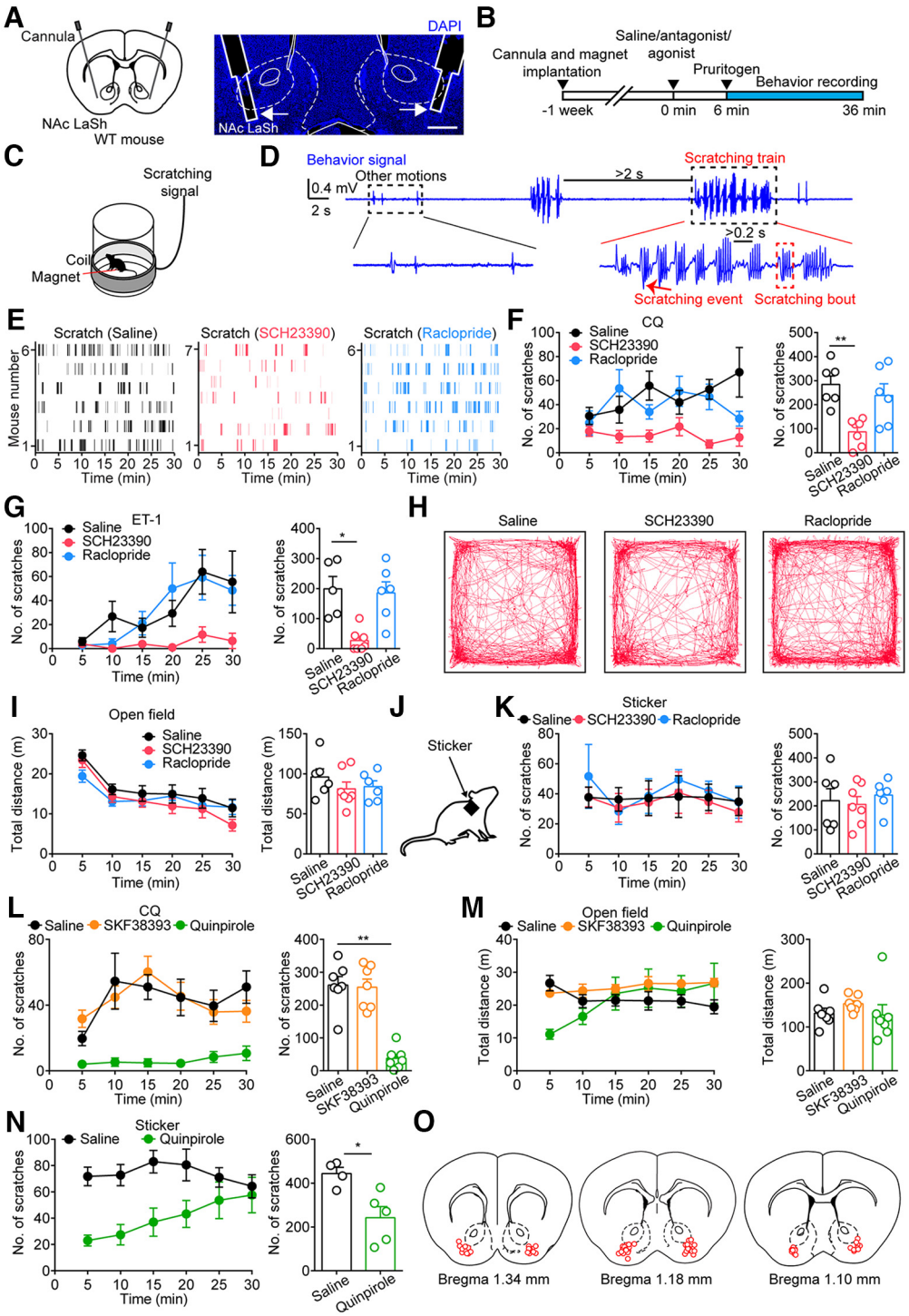

Figure 1. Effects of manipulation of D1R or D2R in the NAc LaSh on scratching behavior. ***A***, Left panel, Schematic of cannula implantation in the NAc LaSh. Right panel, Histologic verification of the location of cannulas in an example animal; arrows indicate the outline of cannulas. Scale bar, 500 μm. ***B***, Timeline of the antagonist injection and scratching behavior test. ***C***, Schematic of the scratching behavior recording chamber. ***D***, Example trace showing the recorded scratching behavior. ***E***, Raster plot showing CQ-induced scratching bouts in the three groups of mice after drug injection. Each bar represents a single scratching bout ($n = 6$–7 mice in each group). SCH23390, the antagonist of D1R; raclopride, the antagonist of D2R. ***F***, Effects of dopamine receptor antagonists on CQ-induced scratching behavior. Left panel, Number of CQ-induced scratching bouts every 5 min after injection of saline, SCH23390 (0.2 μg/μl, 0.5 μl per site), or raclopride (0.2 μg/μl, 0.5 μl per site). Right panel, Total number of CQ-induced scratching bouts within 30 min of injection of saline, SCH23390, or raclopride (one-way ANOVA, $n = 6$–7 mice in each group, SCH23390 $p = 0.008$, raclopride $p = 0.82$). ***G***, Effects of dopamine receptor antagonists on ET-1-induced scratching behavior. Left panel, Number of ET-1-induced scratching bouts every 5 min after injection of saline, SCH23390 (0.2 μg/μl, 0.5 μl per site), or raclopride (0.2 μg/μl, 0.5 μl site). Right panel, Total number of ET-1-induced scratching bouts within 30 min of injection of saline, SCH23390, or raclopride (one-way ANOVA, $n = 5$–7 mice in each group, SCH23390 $p = 0.01$, raclopride $p > 0.99$). ***H***, Locomotion traces of mice that received injection of saline, SCH23390 (0.2 μg/μl, 0.5 μl per site), or raclopride (0.2 μg/μl, 0.5 μl per site) in the open field test. ***I***, Traveling distance in the open field test of mice in the three groups. Left panel, Traveling distance of mice after every 5 min. Right panel, Total traveling distance of mice in three groups (one-way ANOVA, $n = 6$–7 mice in each group). ***J***, Diagram of a mouse with an adhesive sticker. ***K***, Effect of dopamine receptor antagonists on sticker-induced scratching behavior. Left panel, Number of sticker-induced scratching bouts every 5 min after injection of saline, SCH23390 (0.2 μg/μl, 0.5 μl per site), or raclopride (0.2 μg/μl, 0.5 μl per site). Right panel, Total number of sticker-induced scratching bouts within 30 min of injection of saline, SCH23390, or raclopride (one-way ANOVA, $n = 6$–7 mice in each group). ***L***, Effects of dopamine receptor agonists on CQ-induced scratching behavior. Left panel, Number of CQ-induced scratching bouts

Itch behavioral test

The scratching behavior was analyzed as described previously (Inagaki et al., 2002; Mu et al., 2017). Briefly, a magnet (1 mm in diameter, 3 mm in length, ~17 mg) was implanted into the back of the right hindpaw for each mouse under anesthesia at least 5 d before the behavioral tests. Mice were shaved on the back of the neck and individually handled daily for 5 d before the behavioral tests. Mice were intradermally injected with the pruritic compounds chloroquine (200 μg/50 μl) and endothelin-1 (25 ng/50 μl) into the nape of the neck on the ipsilateral side of the hindpaw with a magnet. During behavioral experiments, mice were placed in a chamber surrounded by a coil connected to an amplifier (Shanghai Deayea Technology). Scratching behavior was recorded for 30 min after injection. The scratching behavior was analyzed with custom codes in MATLAB.

Open field test

The spontaneous motor ability of mice was measured in an open field test. Mice were habituated in the testing room for at least 30 min before the test. Freely moving mice were allowed to explore a behavior chamber ($40 \times 40 \times 40\ cm^3$) for 30 min. The movement of the mice was videotaped with a camera (Dahua.Inc). The chambers were cleaned before and between trials. The behavioral parameters (distance and velocity) were analyzed by EthoVision software (Noldus Information Technologies).

Sticker-induced scratching behavior

A sticker removal test was performed to determine the motor ability. The adhesive sticker (1.5×1.5 cm) was placed on the rostral back of the mice. Mice scratched to remove the sticker, and the scratching behavior was recorded with the magnet induction method.

Pharmacological experiment

For *in vivo* pharmacological experiments, the selective D1R antagonist SCH23390 (0.1 μg/side, Sigma), D1R agonist SKF38393 (4 μg/side, Sigma), D2R antagonist raclopride (0.1 μg/side, Sigma), or D2R agonist quinpirole (2 μg/side, Sigma) was intracisternally injected into the NAc LaSh.

Wireless optogenetic stimulation

For optic stimulation in recording and behavior tests, a wireless receiver (Teleopto) was connected to the blue LED, which had been implanted into the spinal cord of mice. Blue light was delivered at 473 nm and 20 mW in a train of 5-ms light pulses at 5, 10, or 20 Hz for 2 s every 30 s. The laser power was measured at the surface of the LED, and the output of the laser was controlled via a Master 9 pulse stimulator (A.M.P.I.).

Imaging

Images of brain slices were acquired by an Olympus VS120 fluorescence microscope with a 10× objective.

Statistical analysis

Statistical analysis was performed by GraphPad Prism 6 and MATLAB 2014a. All analyses were two-tailed comparisons. The data were analyzed using a Mann-Whitney test, Wilcoxon test, Kruskal–Wallis test, and two-way ANOVA. Statistical significance was set at $p < 0.05$, and p values of <0.001 are reported as $p < 0.001$.

Results

Different role of D1R and D2R expressed in the NAc LaSh during itch signal processing

To investigate the functional role of D1R expressed in the NAc LaSh during itch processing, we determined the effect of blocking D1R in the NAc LaSh on itch-induced scratching behavior. We bilaterally implanted cannulas into the NAc LaSh (Fig. 1*A*, *O*). Then, we injected SCH23390, a selective antagonist of D1R, into the bilateral NAc LaSh. Immediately after local injection of SCH23390, we intradermally injected chloroquine (CQ) into the rostral back of mice and recorded the scratching behavior for 30 min with a magnetic induction method (Fig. 1*B–D*; Mu et al., 2017). We found that blocking D1R in the NAc LaSh by local injection of SCH23390 significantly attenuated the scratching behavior induced by CQ (Fig. 1*E*,*F*). We also examined whether the same manipulation affected scratching behavior induced by another pruritogen, endothelin-1 (ET-1), and found that the blockade of D1R in the NAc LaSh also decreased scratching behavior in the ET-1 model (Fig. 1*G*). It has been shown that the activity of D1R in the NAc LaSh is also related to motor control (Baldo et al., 2002; Floresco, 2015). It is thus likely that the reduction in scratching behavior after blockade of D1R in the NAc LaSh is due to a nonspecific effect on motor activity. To examine this possibility, we measured the locomotor activity of mice after infusion of SCH23390 in the NAc LaSh with the open field test. No significant difference was detected in the traveling distance observed between mice injected with saline and those injected with SCH23390 (Fig. 1*H*,*I*), indicating that the blockade of D1R did not affect the locomotion of mice. We recognized that the movements involved in itch-induced scratching were different from those involved in locomotion. Thus, we further examined the effect of blocking D1R in the NAc LaSh on the scratching behavior induced by an adhesive sticker (Fig. 1*J*). The sticker was used as a non-noxious mechanical stimulus (Bradbury et al., 2002; Ranade et al., 2014; Campos et al., 2018) to induce scratching behavior. After the injection of SCH23390, we immediately placed an adhesive sticker on the rostral back of mice and recorded scratching behavior for 30 min. We found that the blockade of D1R in the NAc LaSh did not influence scratching behavior induced by stickers (Fig. 1*K*). These results further support the notion that the attenuation of scratching behavior was not because of motor impairment after blocking D1R. Next, we asked whether pharmacologic activation of D1R could enhance scratching behavior. With a similar approach, we activated D1R in the NAc LaSh by bilateral injection of SKF38393, a selective agonist of D1R. However, activation of D1R in the NAc LaSh did not affect CQ-induced scratching behavior (Fig. 1*L*) or the locomotion of mice in the open field test (Fig. 1*M*). Taken together, our results suggest that activation of D1R in the NAc LaSh is necessary for itch-induced scratching behavior.

D2R is also highly expressed in the NAc, and we asked whether D2R plays roles similar to those of D1R in itch processing. We found that the blockade of D2R in the NAc LaSh by local injection of the selective antagonist of D2R, raclopride, did not affect the scratching behavior induced by pruritogens (Fig. 1*E–G*). In addition, the observed traveling distance of mice injected with saline was similar to that of mice injected with raclopride

←

every 5 min after injection of saline, SKF38393 (8 μg/μl, 0.5 μl per site), or quinpirole (4 μg/μl, 0.5 μl per site). Right panel, Total number of CQ-induced scratching bouts within 30 min of injection of saline, SKF38393, or quinpirole ($n = 7$ mice per group, one-way ANOVA, SKF38393 $p > 0.99$, quinpirole $p = 0.003$). ***M***, Traveling distance in the open field test of mice in the three groups. Left panel, Traveling distance of mice after every 5 min. Right panel, Total traveling distance of mice in three groups ($n = 7$ mice per group, one-way ANOVA, SKF38393 $p = 0.24$, quinpirole $p = 0.88$). ***N***, Effects of dopamine D2 receptor agonist on sticker-induced scratching behavior. Left panel, Number of sticker-induced scratching bouts every 5 min after injection of saline or quinpirole (4 μg/μl, 0.5 μl per site). Right panel, Total number of sticker-induced scratching bouts within 30 min of injection of saline or quinpirole ($n = 4$–5 mice in each group, Mann-Whitney test, $p = 0.03$). ***O***, The locations of the tips of injection tubes in mice. Each red circle represents an injection tube ($n = 40$ mice). All error bars represent SEM; $^*p < 0.05$, $^{**}p < 0.01$.

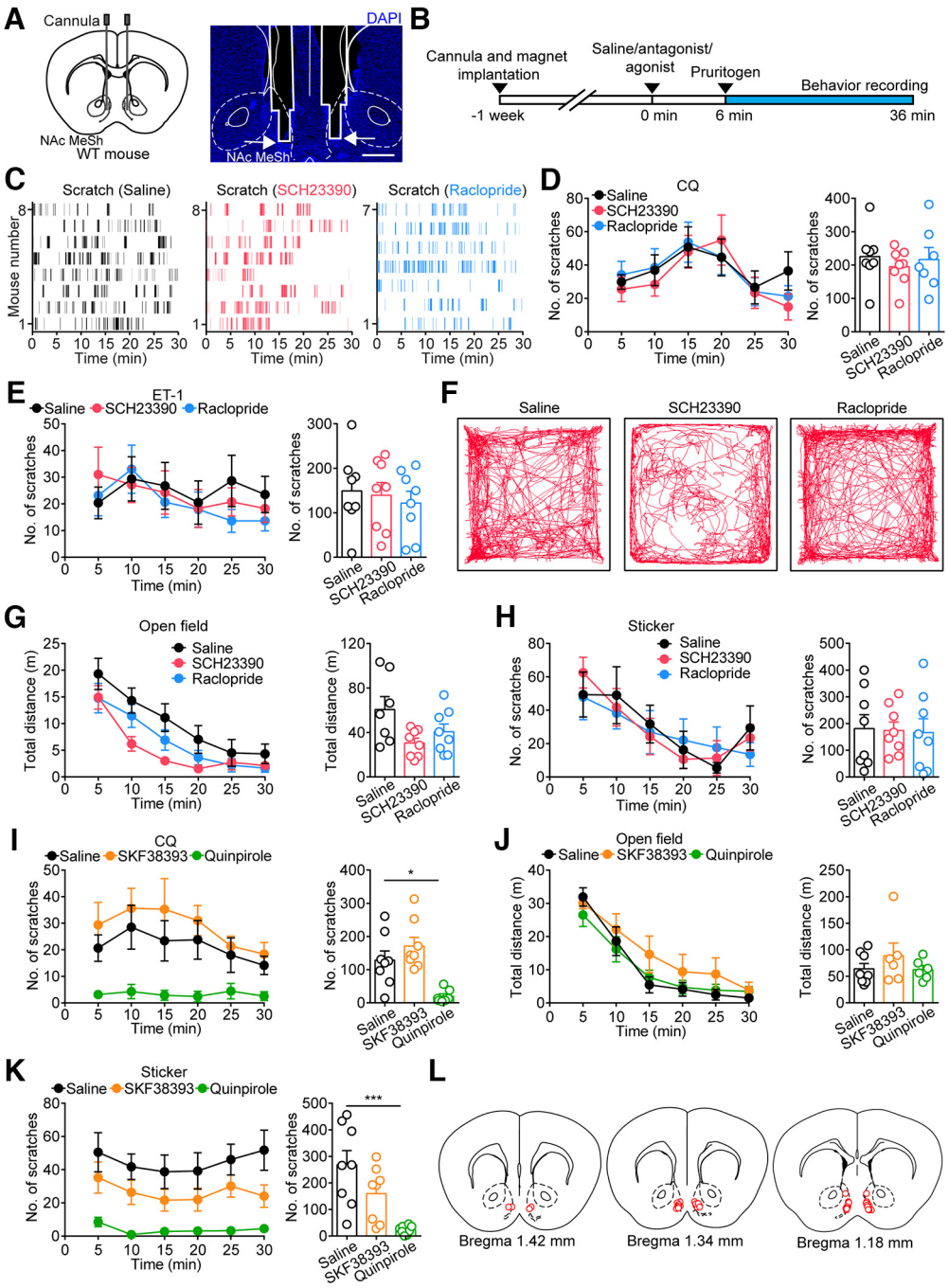

Figure 2. Effects of manipulation of D1R or D2R in the NAc MeSh on scratching behavior. ***A***, Left panel, Schematic of cannula implantation in the NAc MeSh. Right panel, Histologic verification of the location of the cannulas in an example animal; arrows indicate the outline of cannulas. Scale bar, 500 μm. ***B***, Timeline of the antagonist injection and scratching behavior test. ***C***, Raster plot showing CQ-induced scratching bouts detected in three groups of mice after drug injection. Each bar represents a single scratching bout ($n = 7$–8 mice in each group). ***D***, Effects of dopamine receptor antagonists on CQ-induced scratching behavior. Left panel, Number of CQ-induced scratching bouts every 5 min after injection of saline, SCH23390 (0.2 μg/μl, 0.5 μl per site), or raclopride (0.2 μg/μl, 0.5 μl per site). Right panel, Total number of CQ-induced scratching bouts within 30 min after injection of saline, SCH23390, or raclopride ($n = 7$–8 mice in each group, one-way ANOVA, SCH23390 $p = 0.71$, raclopride $p = 0.92$). ***E***, Effects of dopamine receptor antagonists on ET-1-induced scratching behavior. Left panel, Number of ET-1-induced scratching bouts every 5 min after injection of saline, SCH23390 (0.2 μg/μl, 0.5 μl per site), or raclopride (0.2 μg/μl, 0.5 μl per site), Right panel, Total number of ET-1-induced scratching bouts within 30 min after injection of saline, SCH23390, or raclopride ($n = 8$ mice per group, one-way ANOVA, SCH23390 $p > 0.99$, raclopride $p > 0.99$). ***F***, Locomotion traces of mice that received an injection of saline, SCH23390 (0.2 μg/μl, 0.5 μl per site), or raclopride (0.2 μg/μl, 0.5 μl per site) in the open field test. ***G***, Traveling distance in the open field test of mice in the three groups. Left panel, Traveling distance of mice every 5 min. Right panel, Total traveling distance of mice in the three groups ($n = 7$–8 mice in each group, one-way ANOVA, SCH23390 $p = 0.09$, raclopride $p = 0.51$). ***H***, Effects of dopamine receptor antagonists on sticker-induced scratching behavior. Left panel, Number of sticker-induced scratching bouts every 5 min after injection of saline, SCH23390 (0.2 μg/μl, 0.5 μl per site), or raclopride (0.2 μg/μl, 0.5 μl per site). Right panel, Total number of sticker-induced scratching bouts within 30 min after injection of saline, SCH23390, or raclopride ($n = 8$ mice per group, one-way ANOVA, SCH23390 $p > 0.99$, raclopride $p > 0.99$). ***I***, Effects of dopamine receptor agonists on CQ-induced scratching behavior. Left panel, Number of CQ-induced scratching bouts every 5 min after injection of saline, SKF38393 (8 μg/μl, 0.5 μl per site), or quinpirole (4 μg/μl, 0.5 μl per site). Right panel, Total number of CQ-induced scratching bouts within 30 min after injection of saline, SKF38393, or quinpirole ($n = 7$–8 mice in each group, one-way ANOVA, SKF38393 $p = 0.64$, quinpirole $p = 0.02$). ***J***, Traveling distance in the open field test of the three groups. Left panel, Traveling distance of mice every 5 min. Right panel, Total traveling distance of mice in three groups ($n = 6$–8 mice in each group, one-way ANOVA, SKF38393 $p = 0.85$, quinpirole $p > 0.99$). ***K***, Effects of dopamine receptor agonists on sticker-induced scratching behavior. Left panel, Number of sticker-induced

(Fig. 1*H*,*I*). The scratching behavior induced by the adhesive sticker after blocking D2R in the NAc LaSh also showed no difference between the two groups of mice (Fig. 1*K*). We next examined the effect of D2R activation in the NAc LaSh on itch-induced scratching behavior. We found that activation of D2R in the NAc LaSh by bilateral local injection of the D2R-specific agonist quinpirole attenuated the scratching behavior induced by pruritogens (Fig. 1*L*). Moreover, the same dosage of quinpirole did not affect the moving distance in the open field test (Fig. 1*M*) but significantly reduced the sticker-induced scratching behavior (Fig. 1*N*). These results indicate that activation of D2R is sufficient to stop scratching behavior, consistent with previous studies showing that activation of D2R causes a reduction in motor behavior (Mogenson and Wu, 1991; Wu et al., 1993). Taken together, our results suggest that the activation of the dopaminergic signaling pathway through D1R in the NAc LaSh is necessary for itch processing, while scratching behavior is inhibited by the activation of D2R in the NAc LaSh.

D1R and D2R in the NAc MeSh play a negligible role in itch signal processing

Next, we investigated the role of dopamine receptors in the NAc MeSh in itch processing with a pharmacological approach. To determine the role of D1R in the NAc MeSh during itch signal processing, we bilaterally implanted cannulas into the NAc MeSh (Fig. 2*A*,*L*) and blocked D1R by local injection of SCH23390 (Fig. 2*B*). We found that blocking D1R in the NAc MeSh did not affect the scratching behavior induced by CQ (Fig. 2*C*,*D*). Moreover, blocking D1R in the NAc MeSh did not influence the scratching behavior induced by ET-1 (Fig. 2*E*). As a control, we examined the influence on locomotion in the open field test by blocking D1R in the NAc MeSh. There was no significant difference in the total traveling distance between mice injected with saline and those injected with SCH23390, suggesting that the blockade of D1R in the NAc MeSh did not affect locomotion (Fig. 2*F*,*G*). Furthermore, we examined the effect on adhesive sticker-induced scratching behavior after blocking D1R in the NAc MeSh. As expected, we found that blockade of D1R in the NAc MeSh did not influence sticker-induced scratching behavior (Fig. 2*H*). These results indicate that blockade of D1R in the NAc MeSh did not affect the motor ability of mice. Next, we asked whether activation of D1R in the NAc MeSh would affect pruritogen-induced scratching behavior. We activated D1R in the NAc MeSh via local injection of SKF38393. We found that activation of D1R in the NAc MeSh did not affect scratching behavior induced by CQ (Fig. 2*I*). In addition, activation of D1R in the NAc MeSh did not significantly affect the moving distance in the open field test (Fig. 2*J*) or the sticker-evoked scratching behavior (Fig. 2*K*). These results indicate that D1R in the NAc MeSh were not involved in itch information processing.

In addition, we investigated the functional role of D2R in the NAc MeSh in itch processing. We found that blocking D2R in the NAc MeSh by bilateral local injection of raclopride did not affect the scratching behavior induced by pruritogens (Fig. 2*C*–*E*). Furthermore, the blockade of D2R in the NAc MeSh did not affect the traveling distance in the open field test (Fig. 2*F*,*G*) or the scratching behavior induced by adhesive stickers (Fig. 2*H*). We further examined whether the activation of D2R in the NAc MeSh could influence scratching behavior. Consistently, we found that activation of D2R in the NAc MeSh by local injection of quinpirole significantly attenuated the scratching behavior induced by both pruritogens and the sticker (Fig. 2*I*,*K*). However, the same dosage of quinpirole did not significantly affect locomotion (Fig. 2*J*). These results indicate that activation of D2R in the NAc MeSh is sufficient to stop scratching behavior.

Thus, our results suggest that D1R and D2R in the MeSh of the NAc play a negligible role in initiating itch-associated scratching behavior, but activation of D2R in the MeSh of the NAc terminates itch-associated scratching behavior.

Dynamics of dopamine release in the NAc LaSh during itch-induced scratching behavior

We next examined the dynamics of dopamine release in the NAc LaSh during itch-induced scratching behavior by employing a G-protein-coupled receptor-activation-based (GRAB) dopamine sensor (DA2h; Sun et al., 2020), which can detect the changes in concentration of dopamine. We first examined the dopamine release that could be sensed by $D1R^+$ neurons during pruritogen-induced scratching. To achieve this, we selectively expressed DA2h in $D1R^+$ neurons by injecting a Cre-dependent adeno-associated virus (AAV) encoding DA2h into the NAc LaSh in D1-Cre mice. An optical fiber was implanted above the injected site for subsequent measurement of the fluorescent signal of the dopamine sensor (Fig. 3*A*,*B*,*K*). A magnet was implanted into the right hindpaw of mice to record the magnetic electrical signal induced by scratching. We injected CQ intradermally into the rostral back of mice and recorded the dopamine signals and the scratching behavior simultaneously two weeks after surgery (Fig. 3*C*,*D*). We aligned the dopamine signals with the onset of scratching behavior and found that the dopamine signals detected by DA2h expressed in $D1R^+$ neurons in the NAc LaSh increased after scratching onset (Fig. 3*D*,*E*,*I*). In contrast, dopamine release did not change near the scratching offset (Fig. 3*F*,*I*). We also recorded the dopamine signal in the NAc LaSh in the ET-1 model and found that the results were similar to those in the CQ model, in which the dopamine signal increased immediately after the onset of scratching but without robust fluctuations around the scratching offset (Fig. 3*I*). These results indicate that $D1R^+$ neurons in the NAc LaSh received dopamine signals at the beginning of itch-induced scratching behavior.

Next, we measured the dynamics of dopamine signals detected by $D2R^+$ neurons in the NAc LaSh during pruritogen-induced scratching behavior. We found that dopamine signals detected by $D2R^+$ neurons also increased after the onset of scratching (Fig. 3*D*,*G*,*J*), with no significant changes around the offset of scratching (Fig. 3*H*,*J*) in both the CQ and ET-1 models, which was similar to the result from $D1R^+$ neurons (Fig. 3*I*).

Dynamics of dopamine signals in the NAc MeSh during itch-induced scratching behavior

Given that the blockade of D1R or D2R in the NAc MeSh did not affect pruritogen-induced scratching behavior, we wondered what the dynamics of dopamine release in the NAc MeSh are during itch-induced scratching behavior. We examined the dynamics of dopamine signals detected by D1R-expressing or

←

scratching bouts every 5 min after injection of saline, SKF38393 (8 μg/μl, 0.5 μl per site), or quinpirole (4 μg/μl, 0.5 μl per site). Right panel, Total number of sticker-induced scratching bouts within 30 min after injection of saline, SKF38393, or quinpirole ($n = 8$ mice per group, one-way ANOVA, SKF38393 $p = 0.53$, quinpirole $p < 0.001$). ***L***, The locations of the tips of injection tubes in mice. Each red circle represents an injection tube ($n = 24$ mice). All error bars represent SEM; $^*p < 0.05$, $^{***}p < 0.001$.

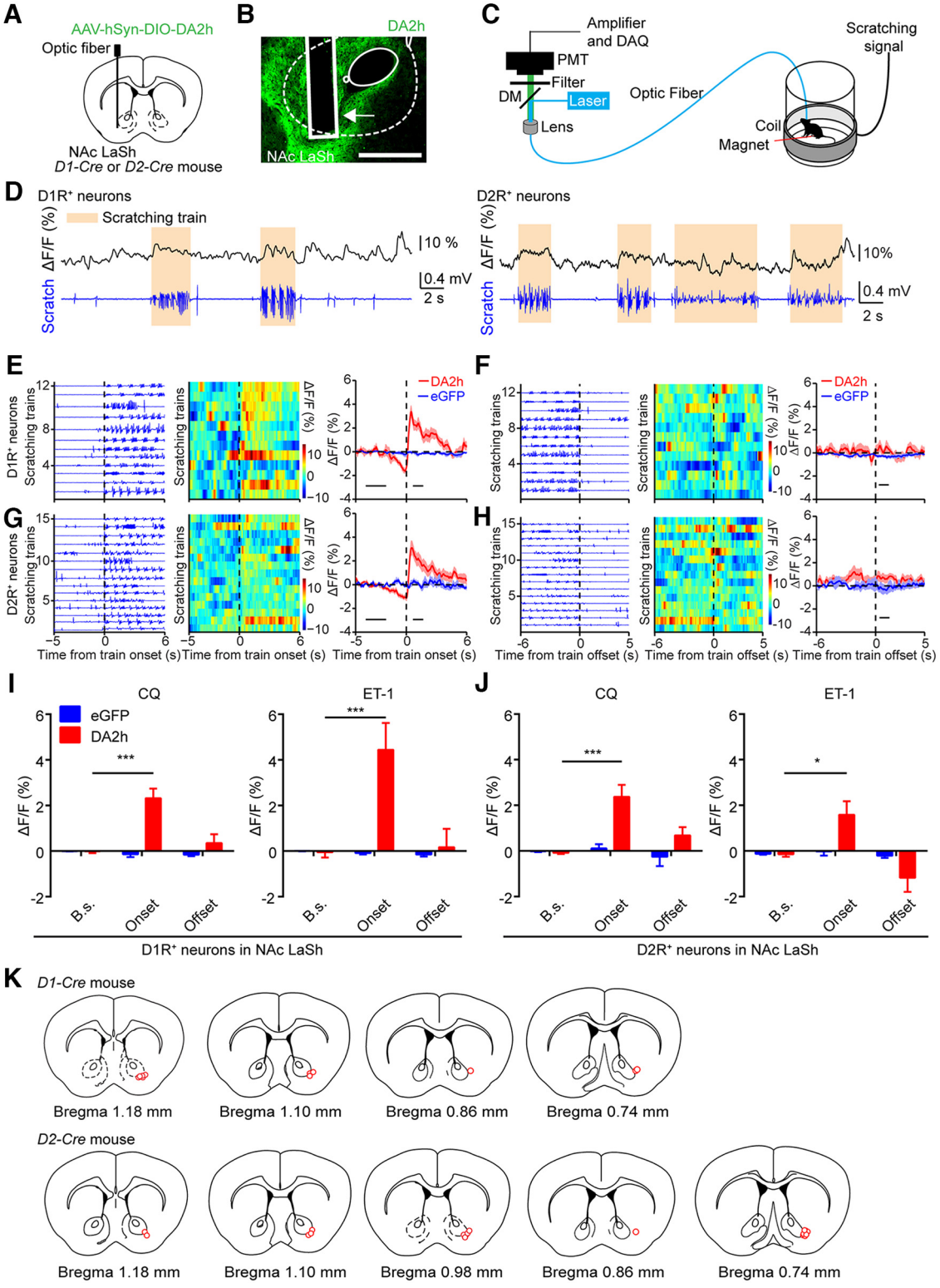

Figure 3. Dopamine release in the NAc LaSh increased during itch-induced scratching behavior. ***A***, Schematic of virus injection and optic fiber implantation in the NAc LaSh. ***B***, Histologic verification of the location of the optic fiber in an example NAc LaSh$^{D1\text{-}DA2h}$ animal. The arrow indicates the outline of the optic fiber. Scale bar, 500 μm. ***C***, Schematic of simultaneous recording of the fluorescence signals of DA2h by fiber photometry during scratching behavior. ***D***, Left panel, Representative DA2h fluorescence trace in NAc LaSh D1R$^+$ neurons (top) and behavioral trace (bottom) in response to an intradermal injection of CQ. Right panel, Representative DA2h fluorescence trace in NAc LaSh D2R$^+$ neurons (top) and behavioral trace (bottom) in response to an intradermal injection of CQ. Yellow shading indicates a scratching train. ***E***, Dopamine signal detected by D1R$^+$ neurons in the NAc LaSh at the onset of the scratching train in an example mouse in response to intradermal injection of CQ. Left panel, Individual scratching train trace aligned to the train onset of an example mouse. Middle panel, Heatmap of the DA2h fluorescence signal during each corresponding scratching train of an example mouse. Right panel, Average fluorescence change of all mice, with shaded area indicating SEM ($n = 11$ mice in DA2h group, $n = 4$ mice in eGFP group). The black bar indicates the baseline (B.s., −4 to −2 s) and the scratching train onset period (Onset, 0.5–1.5 s) used to quantify the fluorescent signal. ***F***, Dopamine signal detected by D1R$^+$ neurons in the NAc LaSh during scratching offset in the CQ model. Left panel, Scratching train trace of an example mouse aligned to the scratching train offset. Middle panel, Heatmap of the DA2h fluorescence signal during each scratching train of the same mouse. Right panel, Average DA2h fluorescence change of the whole group of mice, with

D2R-expressing neurons in the NAc MeSh during itch-induced scratching behavior. We expressed the Cre-dependent AAV encoding a dopamine sensor in the NAc MeSh of D1-cre mice to probe the dynamics of dopamine release during itch-induced scratching behavior (Fig. 4*A–D*,*K*). By aligning the fluorescence signal with the onset and offset of scratching behavior, we found that in the NAc MeSh, dopamine release to $D1R^+$ neurons did not significantly change near the onset or the offset of scratching behavior in different pruritic models (Fig. 4*D–F*,*I*).

We also recorded the dopamine release detected by $D2R^+$ neurons in the NAc MeSh during itch-induced scratching behavior. In both the CQ and ET-1 models, no significant change was observed after the onset of scratching behavior (Fig. 4*G*,*J*). Interestingly, after the offset of scratching, the dopamine signals in the NAc MeSh significantly increased (Fig. 4*H*,*J*). Taken together, there was no elevation of dopamine release during the onset of scratching behavior in the NAc MeSh, but dopamine release sensed by $D2R^+$ neurons was increased at the end of scratching behavior. These results were consistent with the results of manipulation experiments that showed activation of D2R decreased scratching behavior.

Dynamics of dopamine signals in the NAc LaSh under different conditions during itch processing

The circuit information of $D1R^+$ and $D2R^+$ neurons in different subregions of the NAc is interesting; however, a more important question is the potential role of dopamine signals in the NAc during itch processing. Dopaminergic neurons have been implicated in both the motivational component of itch-related scratching behavior and the reward (itch relief) of scratching an itch (Yuan et al., 2018; Su et al., 2019). We further examined the potential role of dopamine signaling in the NAc LaSh. To this end, the timing of the pruritic inputs needed to be precisely controlled. We achieved this goal by optogenetically activating spinal gastrin-releasing peptide receptor (GRPR)-positive neurons, which are identified as the key nodes of spinal itch circuits (Sun and Chen, 2007; Sun et al., 2009; Chen, 2021). Optogenetic activation of cervical spinal $GRPR^+$ neurons induced laser frequency-dependent scratching behavior (Fig. 5*A–F*), indicating that optogenetic manipulation of spinal $GRPR^+$ neurons successfully induced the itch sensation, consistent with recent studies (Liu et al., 2019; Chen et al., 2022). Next, we wondered how to separate the itch sensation and itch relief. Because it is difficult to completely block scratching behavior, activation of cervical spinal $GRPR^+$ neurons is not a suitable model. When a pruritic stimulus is applied to an area that cannot be scratched, mice bite to relieve the itch sensation (Gotoh et al., 2011; Wang et al., 2022). To better dissociate itch sensation and itch relief during itch-induced relieving behavior, we chose to activate lumbar spinal $GRPR^+$ neurons to characterize the itch-induced behavior that was videotaped and analyzed manually (Fig. 5*G–I*), as the pruritic stimulus-evoked biting behavior could be totally blocked by wearing collars (Fig. 5*J*). In this experiment, the animal exhibited body turning and biting behaviors in response to optogenetic activation of spinal $GRPR^+$ neurons. At low stimulation frequencies, not all trials induced turning and biting behaviors. We thus analyzed the induction probability of turning or biting behavior in response to lumbar spinal $GRPR^+$ neuron activation. We found that at a frequency of 5 Hz, over 50% of stimulation trials evoked turning behavior, but very few trials successfully evoked biting behavior. At a frequency of 10 Hz, nearly all trials evoked turning behavior, but less than half of the trials evoked biting behavior. At a frequency of 20 Hz, almost every trial successfully induced biting behavior (Fig. 5*I*).

Given that D1R in the NAc LaSh is critical for itch-evoked scratching behavior, we recorded dopamine signals by expressing the DA sensor in $D1R^+$ neurons of the NAc LaSh while activating lumbar spinal $GRPR^+$ neurons. Our intention with this was to characterize the dynamics of dopamine release detected by $D1R^+$ neurons during the whole precisely controlled itch and itch-relieving cycle. To achieve this, we crossed the *GRPR-Flpo* mouse line with the *D1-Cre* mouse line to obtain a *D1-Cre/GRPR-Flpo* double transgenic mouse line. We labeled spinal $GRPR^+$ neurons with channelrhodopsin-2 (ChR2) by injecting Flpo-dependent AAV encoding ChR2 into the lumbar spinal cord of *D1-Cre/GRPR-Flpo* mice and implanted a blue LED above the injected sites to activate $GRPR^+$ neurons in the spinal cord (Fig. 6*A*,*B*). The Cre-dependent AAV encoding a dopamine sensor was injected into the NAc LaSh of the same animal, followed by implantation of the optic fiber above the injection site to record the fluorescence, which represents the dopamine signal detected by $D1R^+$ neurons (Fig. 6*A*,*B*,*P*).

We aligned the dopamine signals with the onset of opto-itch stimuli. We found that the dopamine signal immediately increased after the onset of $GRPR^+$ neuron activation and persisted at a high level throughout the stimulation period (Fig. 6*C–E*). We also aligned the dopamine signals to the onset of turning and the onset of biting behavior. Dopamine signals increased after the onset of turning but before the onset of biting (Fig. 6*F*). To further examine the potential role of dopamine signals during itch processing, we used collars to temporally separate itch sensation and itch relief as mentioned earlier. We used collars of two different sizes (Fig. 6*G*,*K*). The mice wearing the small collar could bite as usual, but the mice wearing the normal collar could not bite to relieve the itch sensation. We found that at the onset of spinal $GRPR^+$ neuron activation, dopamine signals increased with a comparable scale in both groups of mice wearing

←

shaded area indicating SEM ($n = 11$ mice in DA2h group, $n = 4$ mice in eGFP group). The black bar indicates the scratch train offset period (Offset, 0.25–1.25 s) used to quantify the fluorescence. ***G***, Dopamine signal detected by $D2R^+$ neurons in the NAc LaSh at the onset of the scratching train in an example mouse in response to intradermal injection of ET-1. Left panel, Individual scratching train trace aligned to the train onset of an example mouse. Middle panel, Heatmap of the DA2h fluorescence signal during each corresponding scratching train of an example mouse. Right panel, Average fluorescence change of all mice, with shaded area indicating SEM ($n = 20$ mice in DA2h group, $n = 4$ mice in eGFP group). The black bar indicates the baseline period (B.s., −4 to −2 s) and the scratching train onset period (Onset, 0.5–1.5 s) used to quantify the fluorescent signal. ***H***, Dopamine signal detected by $D2R^+$ neurons in the NAc LaSh during scratching offset in the CQ model. Left panel, Scratching train trace of an example mouse aligned to the scratching train offset. Middle panel, Heatmap of the DA2h fluorescence signal during each scratching train of the same mouse. Right panel, Average DA2h fluorescence change of the whole group of mice, with shaded area indicating SEM ($n = 20$ mice in DA2h group, $n = 4$ mice in eGFP group). The black bar indicates the scratching train offset period (Offset, 0.25–1.25 s) used to quantify the fluorescence. ***I***, Quantification of the average DA2h fluorescence change in NAc LaSh $D1R^+$ neurons during the onset of scratching in the CQ (left panel) and ET-1 (right panel) models (two-way ANOVA, in the CQ model, $p < 0.001$ at onset, $p = 0.60$ at offset; in the ET-1 model, $p < 0.001$ at onset, $p = 0.97$ at offset). ***J***, Quantification of the average DA2h fluorescence change in NAc LaSh $D2R^+$ neurons during the onset of scratching in the CQ (left panel) and ET-1 (right panel) models (two-way ANOVA, in CQ model, $p < 0.001$ at onset, $p = 0.12$ at offset; in ET-1 model, $p = 0.04$ at onset, $p = 0.28$ at offset). All error bars represent SEM; $^*p < 0.05$, $^{***}p < 0.001$. ***K***, The locations of the tips of optic fibers in recorded mice. Each red circle represents an individual animal (D1-Cre $n = 11$ mice, D2-Cre $n = 20$ mice).

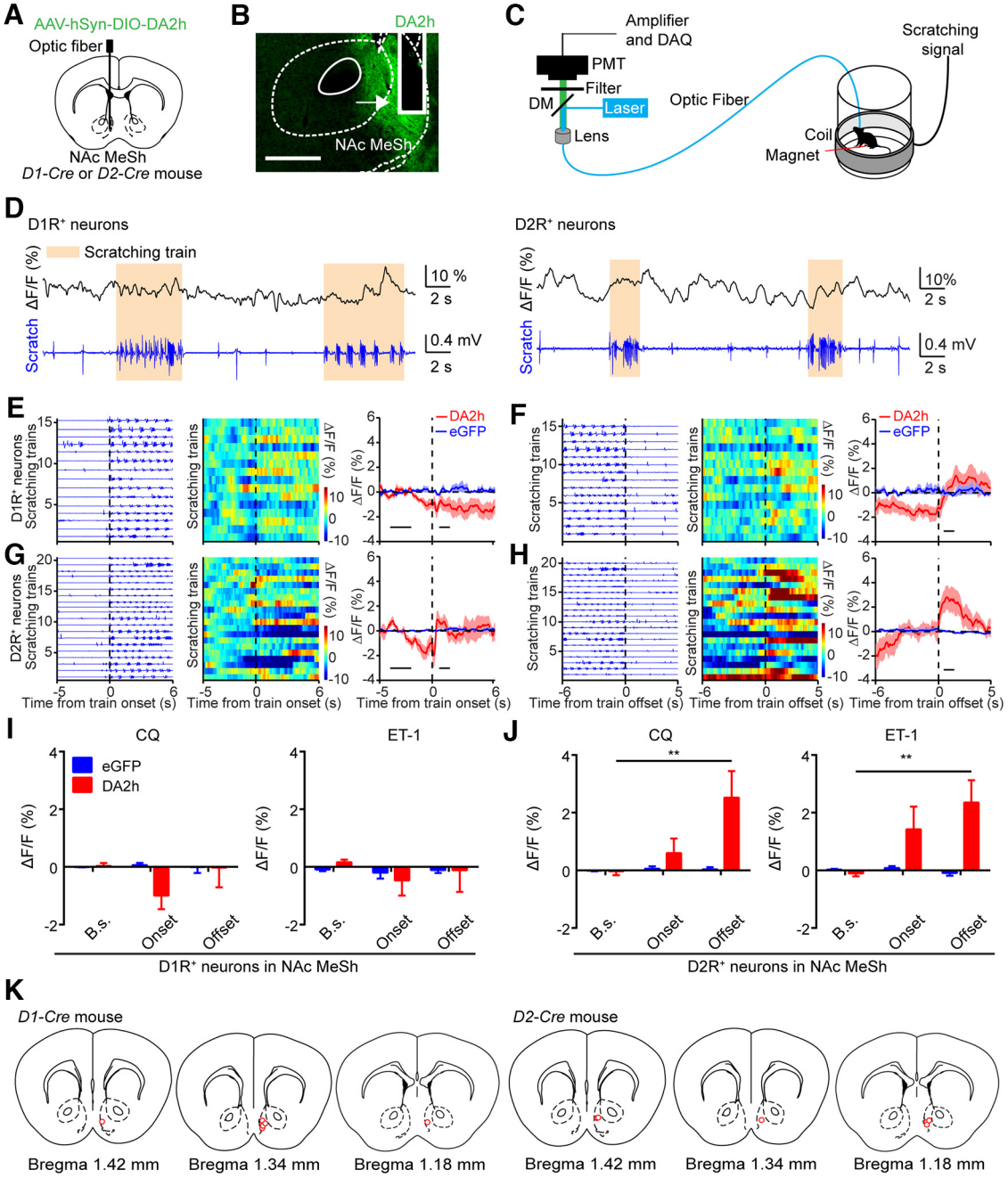

Figure 4. Diverse dynamics of dopamine release in the NAc MeSh during itch-induced scratching behavior. ***A***, Schematic of virus injection and optic fiber implantation in the NAc MeSh. ***B***, Histologic verification of the location of the optic fiber in an example NAc MeSh$^{D1\text{-}DA2h}$ animal. The arrow indicates the outline of the optic fiber. Scale bar, 500 μm. ***C***, Schematic of simultaneous recording of the fluorescence signals of DA2h by fiber photometry during scratching behavior. ***D***, Left panel, Representative DA2h fluorescence trace in NAc MeSh D1R$^+$ neurons (top) and behavioral trace (bottom) in response to an intradermal injection of CQ. Right panel, Representative DA2h fluorescence trace in NAc MeSh D2R$^+$ neurons (top) and behavioral trace (bottom) in response to an intradermal injection of CQ. Yellow shading indicates a scratching train. ***E***, Dopamine signal detected by D1R$^+$ neurons in the NAc MeSh at the onset of the scratching train in an example mouse. Left panel, Individual scratching train trace aligned with the train onset of an example mouse. Middle panel, DA2h fluorescence signal during each corresponding scratching train of an example mouse. Right panel, Average fluorescence change of all mice, with shaded area indicating SEM ($n = 6$ mice in DA2h group, $n = 4$ mice in eGFP group). The black bar indicates the baseline period (B.s., −4 to −2 s) and the scratching train onset period (Onset, 0.5–1.5 s) used to quantify the fluorescent signal. ***F***, Dopamine signal detected by D1R$^+$ neurons in the NAc MeSh during scratching offset in the CQ model. Left panel, Scratching train trace of an example mouse aligned to the scratching train offset. Middle panel, Heatmap of the DA2h fluorescence signal during each scratching train of the same mouse. Right panel, Average DA2h fluorescence change of the whole group of mice, with shaded area indicating SEM ($n = 6$ mice in DA2h group, $n = 4$ mice in eGFP group). The black bar indicates the scratching train offset period (Offset, 0.25–1.25 s) used to quantify the fluorescence. ***G***, Dopamine signal detected by D2R$^+$ neurons in the NAc MeSh at the onset of the scratching train in an example mouse. Left panel, Individual scratching train trace aligned to the train onset of an example mouse. Middle panel, DA2h fluorescence signal during each corresponding scratching train of an example mouse. Right panel, Average fluorescence change of all mice, with shaded area indicating SEM ($n = 6$ mice in DA2h group, $n = 4$ mice in eGFP group). The black bar indicates the baseline period (B.s., −4 to −2 s) and the scratching train onset period (Onset, 0.5–1.5 s) used to quantify the fluorescent signal. ***H***, Dopamine signal detected by D2R$^+$ neurons in the NAc MeSh during scratching offset in the CQ model. Left panel, Scratching train trace of an example mouse aligned to the scratching train offset. Middle panel, Heatmap of the DA2h fluorescence signal during each scratching train of the same mouse. Right panel, Average DA2h fluorescence change of the whole group of mice, with shaded area indicating SEM ($n = 6$ mice in DA2h group, $n = 4$ mice in eGFP group). The black bar indicates the scratching train offset period (Offset, 0.25–1.25 s) used to quantify the fluorescence. ***I***, Quantification of the average DA2h fluorescence change in NAc MeSh D1R$^+$ neurons during the onset of scratching in the CQ (left panel) and ET-1 (right panel)

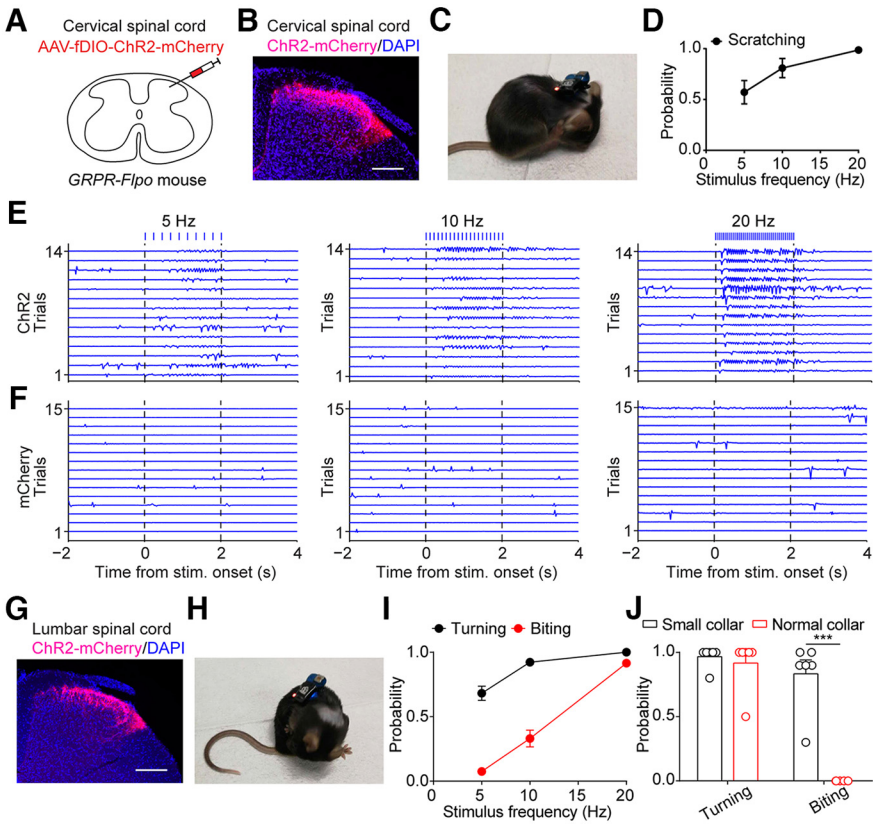

Figure 5. Optostimulation of cervical or lumbar spinal GRPR$^+$ neurons induced scratching or turning and biting behavior. ***A***, Schematic of virus injection in the cervical spinal cord. ***B***, Histologic verification of the expression of the virus encoding ChR2-mCherry in the cervical spinal cord. Scale bar, 200 μm. ***C***, Scratching behavior induced by activation of cervical spinal GRPR$^+$ neurons. ***D***, The probability of successful induction of scratching behavior by different intensities of optogenetic activation of cervical GRPR$^+$ neurons ($n = 10$ mice). ***E***, Optogenetic stimulation of cervical spinal GRPR^{ChR2} neurons induced intensity-dependent scratching behavior. ***F***, Optogenetic stimulation of cervical spinal GRPR^{mCherry} neurons failed to evoke scratching behavior. ***G***, Histologic verification of the expression of the virus encoding ChR2-mCherry in the lumbar spinal cord. Scale bar, 200 μm. ***H***, Biting behavior induced by activation of lumbar spinal GRPR$^+$ neurons. ***I***, The probability of turning or biting behavior induced by different intensities of optogenetic activation of lumbar spinal GRPR$^+$ neurons ($n = 13$ mice). ***J***, Probability of mice turning and biting while wearing collars of different sizes (two-way ANOVA, $p < 0.001$); ***$p < 0.001$.

normal or small collars (Fig. 6*G–N*). We analyzed the dopamine signal during the early phase and the late phase of stimulation. The results showed that dopamine signals from mice wearing small collars and normal collars were similar at the early phase. Interestingly, in the late phase of GRPR$^+$ neuron activation, the dopamine signal was maintained at a high level in mice wearing small collars but returned to baseline in mice wearing normal collars (Fig. 6*O*). These results support the idea that the early phase release of dopamine that targets D1R in the NAc LaSh represents the driving force of itch-relieving behaviors.

Discussion

In this study, we determined distinct roles of different dopamine receptor subtypes in the NAc shell during itch signal processing. We demonstrated that activation of D1R in the NAc LaSh is important for itch signal processing. Our results suggest that dopamine signals in the NAc LaSh are involved in the motivational drive for itch-induced behaviors.

We showed that activation of D1R in the NAc LaSh is necessary for pruritogen-induced scratching behavior. This is demonstrated by the results that blockade of D1R in the NAc LaSh attenuated scratching behavior induced by different pruritogens (Fig. 1). The effect of blocking D1R is not because of motor impairment, as the moving distance in the open field test and sticker-induced scratching were not affected by the same manipulation. Our results are supported by previous studies showing that systemic inhibition of D1R in squirrel monkeys and rats decreased scratching behavior induced by pruritogens (Rosenzweig-Lipson et al., 1994). It is interesting that the scratching behavior evoked by chemical and mechanical stimuli was differentially affected by D1R blockade. Given the important role of D1R in motivation (Bromberg-Martin et al., 2010), it is likely that mechanical stimulation produces less motivational drive to scratch. Thus, the blockade of D1R did not affect sticker-induced scratching behavior. Furthermore, our behavioral results demonstrated that the involvement of D1R in itch processing exhibited subregion specificity. This is supported by the results that blockade of D1R in the NAc MeSh did not affect itch-induced scratching behavior, and that the release of dopamine was elevated in the NAc LaSh but not MeSh during scratching behavior (Figs. 3, 4). We also noticed that locomotion was slightly affected in mice injected with SCH23390 in the NAc MeSh (Fig. 2*G*). However, the total moving distance showed no significant difference between groups, indicating that the influence of motor ability during the whole session was limited. Furthermore, even if the motor ability was mildly affected by SCH23390 injection in NAc MeSh, the same dosage of SCH23390 did not affect the scratching behavior induced by pruritogens. These results are consistent with our conclusion that the NAc MeSh plays a negligible role in itch processing. This subregion specificity of the NAc in itch processing is also consistent with previous observations that NAc subregions are differentially involved in motivational behavior (Aragona et al., 2008; Berridge and Kringelbach, 2015).

In contrast to the blockade of D1R, the blockade of D2R in the NAc shell has no significant effect on scratching behavior during itch. However, the activation of D2R in the NAc shell decreased scratching behavior induced by both pruritic and nonpruritic stimuli, which is consistent with the traditional hypothesis that D2R$^+$ neurons encode the stop signal (Ralph and Caine, 2005; Kravitz et al., 2010; Kai et al., 2015). It is known that the D2R agonist quinpirole also acts on dopamine terminals and

←

models (two-way ANOVA, in the CQ model, $p = 0.09$ at onset, $p = 0.99$ at offset; in the ET-1 model, $p = 0.48$ at onset, $p = 0.86$ at offset). ***J***, Quantification of the average DA2h fluorescence change in NAc MeSh D2R$^+$ neurons during the onset of scratching in the CQ (left panel) and ET-1 (right panel) models (two-way ANOVA, in CQ model, $p = 0.56$ at onset, $p = 0.003$ at offset; in ET-1 model, $p = 0.06$ at onset, $p = 0.004$ at offset). All error bars represent SEM. ***K***, The locations of the tips of optic fibers in recorded mice. Each red circle represents an individual animal (D1-Cre $n = 6$ mice, D2-Cre $n = 6$ mice); **$p < 0.01$.

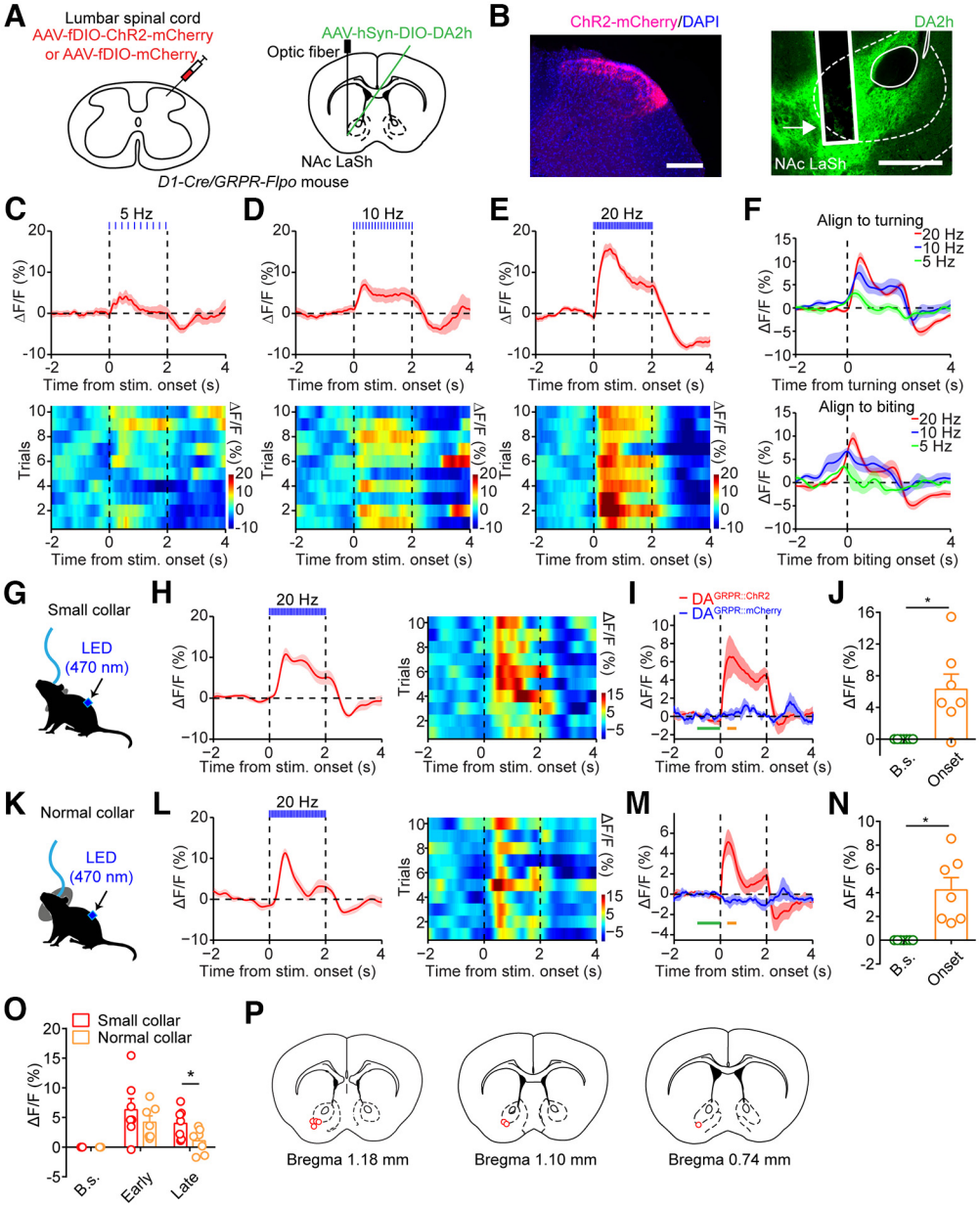

Figure 6. Dopamine release to D1R^{+} neurons in the NAc LaSh did not represent the reward signal accompanied by itch relief. ***A***, Schematic of virus injection in the lumbar spinal cord (left panel) and virus injection and optic fiber implantation in the NAc LaSh (right panel). ***B***, Left panel, Histologic verification of virus expression in the lumbar spinal cord (red: ChR2, blue: DAPI; scale bar, 200 μm). Right panel, Virus expression and optic fiber location in the NAc LaSh. The arrow indicates the outline of the fiber (green: DA2h; scale bar, 500 μm). ***C–E***, Dopamine signals near D1R^{+} neurons in the NAc LaSh during activation of lumbar spinal GRPR^{+} neurons at 5 Hz (***C***), 10 Hz (***D***), and 20 Hz (***E***) optogenetic stimulation in an example mouse. Top panel, Average DA2h dopamine fluorescence signal during each trial of spinal GRPR^{+} neuron activation, with the shaded area indicating the SEM. Bottom panel, Heatmap of each trial. ***F***, Top panel, Average dopamine signal at different intensities aligned to the onset of response behavior (turning), with the shaded area indicating SEM. Bottom panel, Average dopamine signal at different intensities aligned to the onset of itch relief (biting), with the shaded area indicating SEM ($n = 7$ mice in the GRPR^{ChR2} group, $n = 5$ mice in the GRPR^{mCherry} group). ***G***, Diagram of a mouse wearing a small collar during fiber photometry recording. Collar could not block biting or turning behaviors. ***H***, Left panel, Average DA2h fluorescence change of an example mouse wearing a small collar during lumbar spinal GRPR^{+} neuron activation at 20 Hz, with the shaded area indicating SEM. Right panel, Each trial of the example mouse wearing a small collar during spinal GRPR^{+} neuron activation at 20 Hz. ***I***, Average dopamine fluorescence change of mice wearing small collars, with shaded area indicating SEM ($n = 7$ mice). The green bar indicates the baseline period (B.s., −1 to 0 s), and the orange bar indicates the scratch train onset period (Onset, 0.25–0.75 s) that was used to quantify the fluorescent signal. ***J***, Quantification of the dopamine fluorescence signal in mice wearing small collars (Wilcoxon test, $p = 0.03$). ***K,*** Diagram of a mouse wearing a normal collar during fiber photometry recording. ***L***, Left panel, Average DA2h fluorescence change of an example mouse wearing a normal collar during lumbar spinal GRPR^{+} neuron activation at 20 Hz, with the shaded area indicating SEM. Right panel, Each trial of the example mouse wearing a normal collar during spinal GRPR^{+} neuron activation at 20 Hz. ***M***, Average dopamine fluorescence change of mice wearing normal collars, with shaded area indicating SEM ($n = 7$ mice in GRPR^{ChR2} group, $n = 5$ mice in GRPR^{mCherry} group). The green bar indicates the baseline period (B.s., −1 to 0 s), and the orange bar indicates the scratching train onset period (Onset, 0.25–0.75 s) that was used to quantify the fluorescent signal. ***N***, Quantification of dopamine fluorescence signals in mice wearing normal collars (Wilcoxon test, $p = 0.02$). ***O***, Quantification of dopamine fluorescence signals in the early (0.25–0.75 s) and late (1.25–1.75 s) phases during activation of GRPR^{+} neurons of mice wearing small collars and normal collars (two-way ANOVA; B.s., $p > 0.999$; First, $p = 0.12$; Last, $p = 0.02$). ***P***, The locations of the tips of optic fibers in the recorded mice. Each red circle represents an individual animal ($n = 7$ mice). All error bars represent SEM; *$p < 0.05$.

causes a reduction in dopamine release (O'Neill et al., 2009). Therefore, we cannot exclude the possibility that quinpirole injection in the NAc LaSh decreased local dopamine release in the NAc, and D1R could not receive enough dopamine signals to initiate scratching behavior. Our results are consistent with those in rats that activation of D2R nearly abolished pruritogen-induced scratching behavior (Akimoto and Furuse, 2011). However, our data are inconsistent with studies showing that the systemic activation of D2R induced scratching behavior in squirrel monkeys (Pellon et al., 1995). Together, our results demonstrate that the two different dopamine receptor subtypes in the NAc shell are differentially involved in itch processing.

By recording dopamine release with a dopamine sensor, we found that dopamine signals received by the NAc LaSh and MeSh are different in the temporal dimension. $D1R^+$ and $D2R^+$ neurons are intermingled in the NAc and tightly packed together. Given the traditional theory about the volume transmission nature of dopamine, it is reasonable to believe that $D1R^+$ and $D2R^+$ neurons receive dopamine signals with similar temporal properties. It is thus surprising to observe the difference in dopamine signals received by $D1R^+$ and $D2R^+$ neurons in the NAc MeSh at the offset of scratching behavior. This suggests that there is localized dopamine signal transmission in the NAc, although the mechanism needs further investigation. In the NAc LaSh, dopamine release was detected in both $D1R^+$ and $D2R^+$ neurons at the onset of scratching (Fig. 3). A previous study using fiber photometry observed that when animals initiate actions, neural activity transiently increases in both $D1R^+$ and $D2R^+$ neurons (Cui et al., 2013). Manipulation of $D1R^+$ and $D2R^+$ neurons oppositely altered licking behavior during drinking (Z. Chen et al., 2021). These results suggest that these two neuronal subtypes could be involved in the same behavior but play different roles. Dopamine could activate both D1R and D2R during itch processing. We speculate that simultaneous activation of D1R and D2R in the NAc LaSh could coordinate to initiate itch-relieving behavior. Activation of D1R by dopamine might signal the motivational component of scratching, while activation of D2R might assist in suppressing other movements. In contrast, in the NAc MeSh, there was no significant dopamine release at the onset of scratching, and $D2R^+$ neurons in the NAc MeSh receive dopamine signals only at the offset of scratching behavior. A recent study found that the activity of VTA dopaminergic neurons increased ~5 s after the onset of scratching (Su et al., 2019). This likely corresponds to the release of dopamine detected in $D2R^+$ neurons of the NAc MeSh at the offset of scratching. Moreover, we noted that there was a dopamine dip before increase at the onset of scratching behavior. This dip may be because of the inhibition of VTA GABA neurons, which were activated at the beginning of itch-induced scratching (Su et al., 2019).

Dopaminergic neurons in the VTA have been implicated in both motivational and reward components of itch. We precisely controlled the pruritic input by an optogenetic approach. Our study showed that dopamine signals in the NAc LaSh increased before itch-relieving biting behavior, suggesting that dopamine signals in the NAc LaSh might represent motivational signals. This is demonstrated by the data that the dopamine signaling was elevated at the onset of the optogenetic-activation of spinal $GRPR^+$ neurons in mice wearing collars of different sizes. A normal-sized collar could block biting to relieve itch, while mice wearing a small collar could freely bite. Although the itch sensation persisted throughout the activation of $GRPR^+$ neurons, biting can still efficiently relieve itch by causing pain (Han and Dong, 2014). Previous observations that inhibiting the activity of dopaminergic neurons in the VTA at the onset of scratching trains could interrupt scratching (Yuan et al., 2018) also support the hypothesis that dopamine signaling might play a role in driving itch-relieving behavior. Our results differ from a recent study in which a collar was used to block scratching behavior during chronic itch and prevented the elevation of dopamine levels in the NAc after pruritogen application (Setsu et al., 2021). However, that study did not distinguish different NAc subregions and measured dopamine signals by microdialysis, which has poor temporal resolution. In addition, we noticed that the dopamine signal differed in response to the activation of spinal $GRPR^+$ neurons in mice wearing small or normal-sized collars. Sustained dopamine release was detected in the NAc LaSh in mice that could relieve itch by biting, while only transient dopamine release was observed in the NAc LaSh in mice without itch relief. Thus, it remains possible that the dopamine signal in the NAc also represents reward associated with itch relief in late phase. It has been highlighted that dopaminergic neurons respond to both rewarding and aversive stimuli and that salient stimuli in particular can engage the release of dopamine into the NAc (Kutlu et al., 2021). However, the NAc MeSh rather than the NAc LaSh showed a more significant response to aversive stimulation (de Jong et al., 2019). Nevertheless, the dopamine release in the NAc LaSh at the onset of itch stimulation likely represents the motivational component. Although we cannot exclude the possibility that activation of spinal $GRPR^+$ neurons could elicit other sensations, it is conceivable that pruritic input should be dominant during optogenetic activation of spinal $GRPR^+$ neurons (Liu et al., 2019; Chen et al., 2022). Thus, the evidence provided in this study together with previous studies suggests that dopaminergic signals have a role in both the motivation and reward components of itch.

In summary, we found that the D1R and D2R dopamine receptor subtypes play distinct roles in itch, with the D1R expressed in NAc LaSh being critical for itch-evoked scratching behavior. The dopamine signals in the NAc LaSh likely encode the motivational drive for scratching behavior, and D2R activation in the NAc MeSh represents the termination of scratching behavior. Thus, our study reveals the different roles of D1R and D2R in the NAc in itch signal processing.

References

Akimoto Y, Furuse M (2011) SCH23390, a dopamine D1 receptor antagonist, suppressed scratching behavior induced by compound 48/80 in mice. Eur J Pharmacol 670:162–167.

Aragona BJ, Cleaveland NA, Stuber GD, Day JJ, Carelli RM, Wightman RM (2008) Preferential enhancement of dopamine transmission within the nucleus accumbens shell by cocaine is attributable to a direct increase in phasic dopamine release events. J Neurosci 28:8821–8831.

Baldo BA, Sadeghian K, Basso AM, Kelley AE (2002) Effects of selective dopamine D1 or D2 receptor blockade within nucleus accumbens subregions on ingestive behavior and associated motor activity. Behav Brain Res 137:165–177.

Bautista DM, Wilson SR, Hoon MA (2014) Why we scratch an itch: the molecules, cells and circuits of itch. Nat Neurosci 17:175–182.

Beier KT, Steinberg EE, DeLoach KE, Xie S, Miyamichi K, Schwarz L, Gao XJ, Kremer EJ, Malenka RC, Luo L (2015) Circuit architecture of VTA dopamine neurons revealed by systematic input-output mapping. Cell 162:622–634.

Berridge KC, Kringelbach ML (2015) Pleasure systems in the brain. Neuron 86:646–664.
Bradbury EJ, Moon LD, Popat RJ, King VR, Bennett GS, Patel PN, Fawcett JW, McMahon SB (2002) Chondroitinase ABC promotes functional recovery after spinal cord injury. Nature 416:636–640.
Bromberg-Martin ES, Matsumoto M, Hikosaka O (2010) Dopamine in motivational control: rewarding, aversive, and alerting. Neuron 68:815–834.
Campos CA, Bowen AJ, Roman CW, Palmiter RD (2018) Encoding of danger by parabrachial CGRP neurons. Nature 555:617–622.
Castro DC, Bruchas MR (2019) A motivational and neuropeptidergic hub: anatomical and functional diversity within the nucleus accumbens shell. Neuron 102:529–552.
Chen XJ, Liu YH, Xu NL, Sun YG (2021) Multiplexed representation of itch and mechanical and thermal sensation in the primary somatosensory cortex. J Neurosci 41:10330–10340.
Chen XJ, Liu YH, Xu NL, Sun YG (2022) Itch perception is reflected by neuronal ignition in the primary somatosensory cortex. Natl Sci Rev 9: nwab218.
Chen ZF (2021) A neuropeptide code for itch. Nat Rev Neurosci 22:758–776.
Chen Z, Zhang ZY, Zhang W, Xie T, Li Y, Xu XH, Yao H (2021) Direct and indirect pathway neurons in ventrolateral striatum differentially regulate licking movement and nigral responses. Cell Rep 37:109847.
Cui G, Jun SB, Jin X, Pham MD, Vogel SS, Lovinger DM, Costa RM (2013) Concurrent activation of striatal direct and indirect pathways during action initiation. Nature 494:238–242.
de Jong JW, Afjei SA, Pollak Dorocic I, Peck JR, Liu C, Kim CK, Tian L, Deisseroth K, Lammel S (2019) A neural circuit mechanism for encoding aversive stimuli in the mesolimbic dopamine system. Neuron 101:133–151.e7.
Floresco SB (2015) The nucleus accumbens: an interface between cognition, emotion, and action. Annu Rev Psychol 66:25–52.
Gotoh Y, Omori Y, Andoh T, Kuraishi Y (2011) Tonic inhibition of allergic itch signaling by the descending noradrenergic system in mice. J Pharmacol Sci 115:417–420.
Han L, Dong X (2014) Itch mechanisms and circuits. Annu Rev Biophys 43:331–355.
Inagaki N, Igeta K, Kim JF, Nagao M, Shiraishi N, Nakamura N, Nagai H (2002) Involvement of unique mechanisms in the induction of scratching behavior in BALB/c mice by compound 48/80. Eur J Pharmacol 448:175–183.
Kai N, Nishizawa K, Tsutsui Y, Ueda S, Kobayashi K (2015) Differential roles of dopamine D1 and D2 receptor-containing neurons of the nucleus accumbens shell in behavioral sensitization. J Neurochem 135:1232–1241.
Kravitz AV, Freeze BS, Parker PR, Kay K, Thwin MT, Deisseroth K, Kreitzer AC (2010) Regulation of parkinsonian motor behaviours by optogenetic control of basal ganglia circuitry. Nature 466:622–626.
Kutlu MG, Zachry JE, Melugin PR, Cajigas SA, Chevee MF, Kelly SJ, Kutlu B, Tian L, Siciliano CA, Calipari ES (2021) Dopamine release in the nucleus accumbens core signals perceived saliency. Curr Biol 31:4748–4761.e8.
Lammel S, Hetzel A, Häckel O, Jones I, Liss B, Roeper J (2008) Unique properties of mesoprefrontal neurons within a dual mesocorticolimbic dopamine system. Neuron 57:760–773.
Liu MZ, Chen XJ, Liang TY, Li Q, Wang M, Zhang XY, Li YZ, Sun Q, Sun YG (2019) Synaptic control of spinal GRPR(+) neurons by local and long-range inhibitory inputs. Proc Natl Acad Sci U S A 116:27011–27017.
Merali Z, Piggins H (1990) Effects of dopamine D1 and D2 receptor agonists and antagonists on bombesin-induced behaviors. Eur J Pharmacol 191:281–293.
Meyer ME, Van Hartesveldt C, Potter TJ (1993) Locomotor activity following intra-accumbens microinjections of dopamine D1 agonist SK&F 38393 in rats. Synapse 13:310–314.
Mochizuki H, Tanaka S, Morita T, Wasaka T, Sadato N, Kakigi R (2014) The cerebral representation of scratching-induced pleasantness. J Neurophysiol 111:488–498.
Mogenson GJ, Wu M (1991) Effects of administration of dopamine D2 agonist quinpirole on exploratory locomotion. Brain Res 551:216–220.
Morales M, Margolis EB (2017) Ventral tegmental area: cellular heterogeneity, connectivity and behaviour. Nat Rev Neurosci 18:73–85.
Mu D, Deng J, Liu KF, Wu ZY, Shi YF, Guo WM, Mao QQ, Liu XJ, Li H, Sun YG (2017) A central neural circuit for itch sensation. Science 357:695–699.
O'Neill C, Evers-Donnelly A, Nicholson D, O'Boyle KM, O'Connor JJ (2009) D2 receptor-mediated inhibition of dopamine release in the rat striatum in vitro is modulated by CB1 receptors: studies using fast cyclic voltammetry. J Neurochem 108:545–551.
Papoiu AD, Nattkemper LA, Sanders KM, Kraft RA, Chan YH, Coghill RC, Yosipovitch G (2013) Brain's reward circuits mediate itch relief. a functional MRI study of active scratching. PLoS One 8:e82389.
Pellon R, Flores P, Alling K, Witkin JM, Katz JL (1995) Pharmacological analysis of the scratching produced by dopamine D-2 agonists in squirrel-monkeys. J Pharmacol Exp Ther 273:138–145.
Ralph RJ, Caine SB (2005) Dopamine D1 and D2 agonist effects on prepulse inhibition and locomotion: comparison of Sprague-Dawley rats to Swiss-Webster, 129X1/SvJ, C57BL/6J, and DBA/2J mice. J Pharmacol Exp Ther 312:733–741.
Ranade SS, Woo SH, Dubin AE, Moshourab RA, Wetzel C, Petrus M, Mathur J, Bégay V, Coste B, Mainquist J, Wilson AJ, Francisco AG, Reddy K, Qiu Z, Wood JN, Lewin GR, Patapoutian A (2014) Piezo2 is the major transducer of mechanical forces for touch sensation in mice. Nature 516:121–125.
Rosenzweig-Lipson S, Hesterberg P, Bergman J (1994) Observational studies of dopamine D1 and D2 agonists in squirrel monkeys. Psychopharmacology (Berl) 116:9–18.
Russo SJ, Nestler EJ (2013) The brain reward circuitry in mood disorders. Nat Rev Neurosci 14:609–625.
Setsu T, Hamada Y, Oikawa D, Mori T, Ishiuji Y, Sato D, Narita M, Miyazaki S, Furuta E, Suda Y, Sakai H, Ochiya T, Tezuka H, Iseki M, Inada E, Yamanaka A, Kuzumaki N, Narita M (2021) Direct evidence that the brain reward system is involved in the control of scratching behaviors induced by acute and chronic itch. Biochem Biophys Res Commun 534:624–631.
Su XY, Chen M, Yuan Y, Li Y, Guo SS, Luo HQ, Huang C, Sun W, Li Y, Zhu MX, Liu MG, Hu J, Xu TL (2019) Central processing of itch in the midbrain reward center. Neuron 102:858–872.e5.
Sun YG, Chen ZF (2007) A gastrin-releasing peptide receptor mediates the itch sensation in the spinal cord. Nature 448:700–703.
Sun F, Zhou J, Dai B, Qian T, Zeng J, Li X, Zhuo Y, Zhang Y, Wang Y, Qian C, Tan K, Feng J, Dong H, Lin D, Cui G, Li Y (2020) Next-generation GRAB sensors for monitoring dopaminergic activity in vivo. Nat Methods 17:1156–1166.
Sun YG, Zhao ZQ, Meng XL, Yin J, Liu XY, Chen ZF (2009) Cellular basis of itch sensation. Science 325:1531–1534.
Wang B, Wu H, Qi H, Li H, Pan L, Li L, Zhang K, Yuan M, Wang Y, Qiu HJ, Sun Y (2022) Histamine is responsible for the neuropathic itch induced by the pseudorabies virus variant in a mouse model. Viruses 14:1067.
Wu M, Brudzynski SM, Mogenson GJ (1993) Functional interaction of dopamine and glutamate in the nucleus accumbens in the regulation of locomotion. Can J Physiol Pharmacol 71:407–413.
Yang H, de Jong JW, Tak Y, Peck J, Bateup HS, Lammel S (2018) Nucleus accumbens subnuclei regulate motivated behavior via direct inhibition and disinhibition of VTA dopamine subpopulations. Neuron 97:434–449.e4.
Yuan L, Liang TY, Deng J, Sun YG (2018) Dynamics and functional role of dopaminergic neurons in the ventral tegmental area during itch processing. J Neurosci 38:9856–9869.
Yuan L, Dou YN, Sun YG (2019) Topography of reward and aversion encoding in the mesolimbic dopaminergic system. J Neurosci 39:6472–6481.